Pergamon

Solid-State Electronics Vol. 42, No. 6, pp. 943–949, 1998

Printed in Great Britain

PII: S0038-1101(97)00267-0

0038-1101/98 $19.00 + 0.00

A SIMPLE APPROACH TO THE CAPACITANCE TECHNIQUE FOR DETERMINATION OF INTERFACE STATE DENSITY OF A METAL–SEMICONDUCTOR CONTACT

SANTOSH PANDEY and S. KAL

Department of Electronics and Electrical Communication Engineering, Indian Institute of Technology, Kharagpur 721302, India

(Received 28 July 1997; in revised form 10 October 1997)

Abstract—In this study we attempt to interpret the experimentally observed nonideal Al–pSi Schottky diode *I–V* and *C–V* characteristics. The expressions for the capacitance–voltage relationship at low frequency and high frequency are derived considering two non idealities, namely interface states and series resistance. After extracting the diode parameters from the *I–V* and *C–V* characteristics, theoretical plots for the high frequency and low frequency capacitance are obtained using the expressions derived. A comparison of the latter with available experimental plots reveals that the expressions for the low frequency and high frequency capacitance derived here are simpler, more accurate and closer to experimental results than those used in the past. The variation of interface state density with the applied bias voltage is obtained from the low frequency and high frequency *C–V* plots by using the capacitance technique. To examine the validity of the present approach, the value of density of interface states is compared with that obtained by the multifrequency admittance method. It is observed that there is good agreement between the results obtained by both methods. © 1998 Elsevier Science Ltd. All rights reserved

NOTATION

A	Cross-section of the diode (cm^3)
A^*	Richardson constant
C	diode capacitance (F cm^{-2})
C_{LF}	Low frequency capacitance (F cm^{-2})
C_{HF}	High frequency capacitance (F cm^{-2})
D_{it}	Density of interface states (cm^{-2} eV^{-1})
c_1	A constant defined as per Equation (6) (V)
c_2, α	Constants defined as per Equation (6) (dimensionless)
E_g	Energy bandgap of Si (J)
I	Diode current (A)
N_A	Doping concentration (cm^{-3})
q	Electronic charge (C)
Q_{sc}	Space charge density (C cm^{-2})
Q_{it}	Interface state charge density (C cm^{-2})
Q_m	Charge density in the metal (C cm^{-2})
R_s	Series resistance (Ω)
T	Temperature (K)
V	Applied bias voltage (V)
V_0	Voltage intercept defined by Equation (11) (V)
v_p	Difference between Si Fermi level and valence band (V)
ϕ_B	Approximate barrier height (V)
ϕ_0	Neutral level (V)
ϕ_m	Metal work function (V)
β	A constant defined as per Equation (10) (dimensionless)
δ	Oxide thickness (cm)
Δ	Potential drop across oxide layer (V)
χ	Electron affinity of Si (V)
ϵ_s	Permittivity of Si (CV^{-1} cm^{-1})
ϵ_i	Permittivity of the oxide (CV^{-1} cm^{-1})
ψ_s	Surface potential (V)

1. INTRODUCTION

Schottky barrier diodes have been studied extensively in the past and various methods have been proposed for the determination of the different parameters of these devices[1–20]. Several possible factors cause deviations of the ideal diode behaviour and must be taken into account apart from the voltage-dependent image force lowering of the effective barrier height which is most important in the reverse bias range. These include effects of the presence of the oxide layer, variation of the interface charge (or interface density) with applied voltage, series resistance R_s, variations in the effective contact area with depletion layer width, traps within the depletion region. The nonideal capacitance–voltage (*C–V*) and current–voltage (*I–V*) characteristics are especially strongly affected by the interfacial layer and the series resistance.

In Ref.[1], Vasudev suggested a simple graphical method for the determination of a quantity called the excess capacitance C_0, which plays the role of a lumped parameter incorporating most of the nonideality effects in the experimental nonlinear C^{-2} *vs* V plots. Extracting C_0 from the measured capacitance gives a linear plot of $(C–C_0)^{-2}$ *vs* V.

The first studies on the interfacial layer in Schottky diodes were made by Cowley and Sze[2] who obtained their estimation from an analysis of the barrier height with different metallisation as a function of the metal work function. Tseng and Wu[5] discussed the occupation of the interfacial states as a function of applied voltage and extracted

the density distribution of the interface states from the nonideal I–V characteristics. Although a good fit between the theoretical model and the above experiments has been demonstrated[6], the existing simple interfacial model is not sufficient to interpret the C–V observation on the excess capacitance caused by interface states which are in quasi-equilibrium with the semiconductor for forward-biased Schottky barrier diodes. The electrical properties of interface states are characterised by their density, their position in the energy gap and their capture cross-section[7].

In the presence of series resistance, the C–V characteristics exhibit a peak which depends on many parameters such as doping, interface state density and oxide thickness. Several techniques have been proposed[10,11] to determine the interface state density of the metal–semiconductor contact taking into account the interfacial oxide layer and series resistance of the device. The capacitance technique[11] does not require any prior information on the series resistance of the device, considers the presence of the interface layer and only requires the low frequency and high frequency nonideal C–V plots of the Schottky barrier diode for the determination of the interface state density.

Here we discuss the nature of the C–V plots taking into account the various nonidealities such as interface states and series resistance. In Section 2, the basic equations are derived and the effect of interface state on the C–V characteristics is discussed (neglecting series resistance effect). The nonideality due to both series resistance and interface states is dealt with in Section 3. The low frequency and high frequency capacitance expressions are derived and consequently the expression for the interface state density is obtained. The variation of interface state density with the applied voltage of Al–pSi Schottky diode has been determined using the present model and experimental I–V and C–V plots available in the literature. The results are discussed in Section 4. The interface state density distribution extracted from the capacitance technique is compared with that measured from the multifrequency admittance method[12,13].

2. BASIC EQUATIONS

The capacitance of a Schottky barrier diode in the ideal case given by

$$C = \{(q\epsilon_s N_A)/2(\psi_s - V)\}^{1/2}, \tag{1}$$

where N_A is doping concentration, ψ_s is the surface potential and V is the applied forward voltage. From Equation (1), $C^{-2} = 2(\psi_s - V)/(q\epsilon_s N_A)$. As seen from this expression the C^{-2} *vs* V plot is a straight line with a voltage intercept of ψ_s. This idealized situation is often disturbed due to the presence of oxide layer, interface states, interface charges and series resistance. Because of these factors, the C–V plot differs significantly from the ideal case[20].

The effect of interface states on the C–V characteristics of Schottky diode at high frequency is considered below. Figure 1 shows the energy band diagram of a metal–semiconductor system with an interfacial oxide layer. In the figure Φ_m represents the work function of the metal, Δ the potential drop across the oxide layer and positive signs represent fixed charges in the oxide layer. The effect due to series resistance is considered in Section 3. The interface state charge density is given by

$$Q_{it} = -qD_{it}(q\psi_s + qv_p - q\phi_0), \tag{2}$$

where D_{it} is the density of acceptor-like interface states.

The space charge density is given by

$$Q_{sc} = -[2q\epsilon_s N_A \psi_s]^{1/2} \text{ C/cm}^2. \tag{3}$$

From the charge neutrality condition, we get $Q_m = -(Q_{sc} + Q_{it})$ where Q_m is the charge density that appears in the metal. From Fig. 1, the potential Δ across the interface layer is

$$\Delta = -[E_g/q + \chi - \psi_s - v_p - V - \phi_m + IR_s]. \tag{4a}$$

Also, it follows from Gauss Law that

$$\Delta = -\delta Q_m/\epsilon_i, \tag{4b}$$

where δ is the oxide thickness, ϵ_i is the permittivity of the oxide layer.

Equating Equations (4a)–(b),

$$(\delta/\epsilon_i)[Q_{it} + Q_{sc}] = -[E_g/q + \chi - \psi_s - v_p - V - \phi_m + IR_s].$$

From Equations (2) and (3),

$$-(\delta/\epsilon_i)[q^2 D_{it}(\psi_s + v_p - \phi_0) + (2q\epsilon_s N_A \psi_s)^{1/2}] = -[E_g/q + \chi - \psi_s - v_p - V - \phi_m + IR_s]. \tag{5}$$

Introducing the quantities α, c_1, c_2

$$\alpha = q^2 \delta D_{it}/\epsilon_i \text{ (dimensionless)},$$

$$c_1 = 2q\epsilon_s N_A \delta^2/\epsilon_i^2,$$

$$c_2 = 1/(1+\alpha) = \epsilon_i/(\epsilon_i + q^2 \delta D_{it}). \tag{6}$$

Neglecting the series resistance effect for the time being, Equation (5) can be solved for ψ_s[15] as

$$\psi_s(V) = \phi_B - c_2 V - v_p + [c_2^2 c_1/2 - (1/2) \times \{4c_2^2 c_1(\phi_B - c_2 V - v_p) + c_2^4 c_1^2\}^{1/2}],$$

where

$$\phi_B = c_2(E_g/q + \chi - \phi_m) + (1 - c_2)\phi_0. \tag{7}$$

For low doping concentration (*i.e.* low value of c_1),

$$\psi_s(V) = \Phi_B - c_2 V - v_p. \tag{8}$$

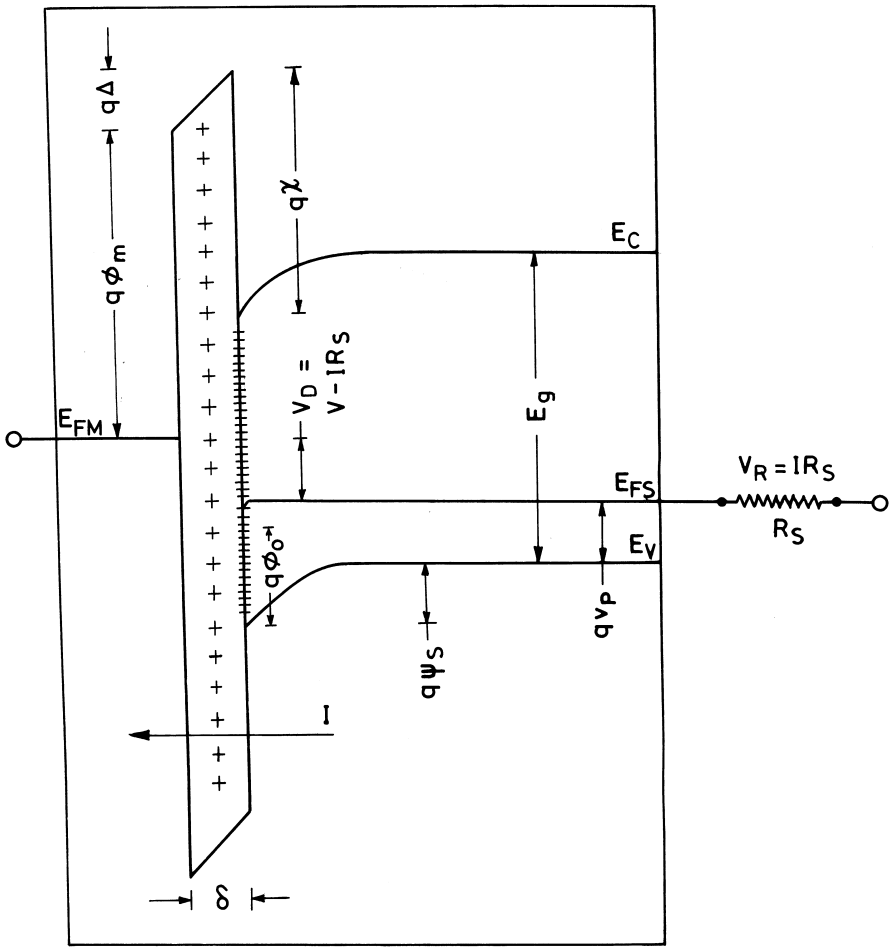

Fig. 1. Energy band diagram of a Schottky barrier diode with an interfacial oxide layer and a series resistance

Now at high frequency, the capacitance of the Schottky barrier diode is the space charge capacitance only. At such a frequency, the charge at the interface states cannot follow the ac signal, so the capacitance due to interface states is zero.

$$C = (\mathrm{d}Q_{\mathrm{sc}}/\mathrm{d}\psi_{\mathrm{s}}) \cdot (\mathrm{d}\psi_s/\mathrm{d}V).$$

From Equations (3) and (8),

$$C = c_2\{(q\epsilon_{\mathrm{s}}N_{\mathrm{A}})/2(\phi_{\mathrm{B}} - c_2V - v_{\mathrm{p}})\}^{1/2} \qquad (9)$$

or

$$1/C^2 = 2(\phi_{\mathrm{B}} - c_2V - v_{\mathrm{p}})/(c_2^2q\epsilon_{\mathrm{s}}N_{\mathrm{A}}).$$

This expression shows that the C^{-2} *vs* V plot is linear and its slope gives the value of c_2.

Usually at the semiconductor interface, there are various kinds of states with different time constants. So at a medium frequency only some of them (βQ_{it}) follow the ac signal, where the parameter β is a function of frequency such that $\beta(0) = 1$ and $\beta(\infty) = 0$. In this case the capacitance is given by $C = \mathrm{d}(Q_{\mathrm{sc}} + \beta Q_{\mathrm{it}})/\mathrm{d}V$.

Using Equations (2), (3) and (8), the capacitance is found to be

$$C = m(\beta)(V_0 - V)^{-1/2} + n(\beta), \qquad (10)$$

where

$$m(\beta) = [1 - \beta(1 - c_2)](q\epsilon_{\mathrm{s}}N_{\mathrm{A}}c_2/2)^{1/2},$$

$$n(\beta) = \beta c_2 q^2 D_{\mathrm{it}},$$

$$V_0 = (\phi_{\mathrm{b}}/q - v_{\mathrm{p}})/c_2. \qquad (11)$$

V_0 is the intercept voltage at high frequency. In this case, if the capacitance measured at any frequency is plotted *vs* $(V_0 - V)^{-1/2}$, we get a straight line but the C^{-2} *vs* V plot is nonlinear. The interface state parameters can be obtained by carrying out the capacitance measurements at two different frequencies[16]: One high, one medium. At high frequency, $\beta = 0$, so $C = (\mathrm{d}Q_{\mathrm{sc}}/\mathrm{d}V)$. Using this value β, $n(\beta) = 0$ and $m(\beta) = (q\epsilon_sN_Ac_2/2)^{1/2}$, then Equation (10) reduces to

$$C = (q\epsilon_{\mathrm{s}}N_{\mathrm{A}}c_2/2)^{1/2}(V_0 - V)^{-1/2}, \qquad (12)$$

which is identical to Equation (9), where V_0 is defined by Equation (11).

3. DETERMINATION OF INTERFACE STATE DENSITY

The capacitance–voltage relationship at high frequency considering the effect of both the series resistance and interface states is derived below. Proceeding from Equation (5) and putting the values of c_1 and c_2 from Equation (6) we get

$$c_2(c_1\psi_s)^{1/2} = c_2(E_g/q + \chi - \phi_m) + (1 - c_2)\phi_0 - c_2V + c_2IR_s - \psi_s - v_p, \quad (13)$$

where R_s is the series resistance of the diode.

The current equation is

$$I = AA^*T^2 \exp[-\{q(\psi_s + v_p)/kT + \phi^{1/2}\delta\}], \quad (14)$$

where ϕ represents the oxide mean barrier. It follows from Equation (14) that

$$dI/d\psi_s = (-q/kT)I \quad (15)$$

Differentiating Equation (13) w.r.t. V and using Equation (15),

$$d\psi_s/dV = c_2/[c_1c_2/2(c_1\psi_s)^{1/2} + 1 + qR_sc_2I/kT]. \quad (16)$$

At high frequency, the capacitance of the device (the parallel component of the impedance of the system) C_{HF} is determined primarily by the depletion capacitance which is frequency independent.

So in this case,

$$C_{HF} = (dQ_{sc}/d\psi_s) \cdot (d\psi_s/dV)$$

Using Equation (3) and Equation (16), the high frequency capacitance is derived as:

$$C_{HF} = \frac{c_2[q\epsilon_sN_A/2\psi_s]^{1/2}}{c_1c_2/2(c_1\psi_s)^{1/2} + 1 + qR_sc_2I/kT}. \quad (17)$$

It is observed that if $R_s = 0$ and $\delta \approx 0$ ($c_1 \approx 0$), then Equation (17) reduces to Equation (9). The presence of the last term in the denominator of Equation (17) leads to a peak in the forward C–V characteristics. This term is significantly small for low current density. If the current density is high, the effect of series resistance becomes prominent.

A similar expression for the high frequency capacitance has been derived in Ref.[11] by a different method. This expression is reproduced here for comparison with Equation (17)

$$C_{HF} = \frac{[q\epsilon_sN_A/2\psi_s]^{1/2}}{\delta(q\epsilon_sN_A/2\psi_s)^{1/2}/\epsilon_i + 1 + qR_sI/kT}. \quad (18)$$

Comparing Equation (18) with Equation (17), we see that Equation (17) reduces to Equation (18) only when $c_2 = 1$. In Ref.[11] the term c_2 in the high frequency capacitance expression has been neglected. But as may be seen from Equation (17) that besides parameters such as doping and series resistance, the capacitance of the device is influenced by the parameter c_2 which is a function of the oxide thickness and interface state density. Measured C–V plots of Schottky barrier diodes in Ref.[9] clearly reflect the role of c_2. For a fixed value of R_s, the peak value of the capacitance increases with c_2. This suggests that series resistance is not the only parameter which influences the C–V plots of a Schottky diode. The presence of the term c_2 is not only shown in Equation (17) but also in Equation (9) and Equation (10).

At low frequency, the interface states do respond to the ac signal. So, here the capacitance of the device can be written as

$$C_{LF} = (dQ_{sc}/d\psi_s) \cdot (d\psi_s/dV) + (dQ_{it}/d\psi_s) \cdot (d\psi_s/dV) = [dQ_{sc}/d\psi_s + dQ_{it}/d\psi_s] \cdot (d\psi_s/dV) \quad (19)$$

where $dQ_{it}/d\psi_s$ represents interface state capacitance. D_{it} is assumed to be independent of ψ_s in order to obtain the solution in closed form. Thus at low frequency, following from Refs.[7,17].

$$dQ_{it}/d\psi_s = qD_{it} \quad (20)$$

From Equations (3), (16) and (20), we get

$$C_{LF} = \frac{[(q\epsilon_sN_A/2\psi_s)^{1/2} + qD_{it}]c_2}{c_1c_2/2(c_1\psi_s)^{1/2} + 1 + qc_2R_sI/kT}. \quad (21)$$

The expression for low frequency capacitance obtained in Ref.[11] is

$$C_{LF} = \frac{[(q\epsilon_sN_A/2\psi_s)^{1/2} + qD_{it}]}{\delta(q\epsilon_sN_A/2\psi_s)^{1/2}/\epsilon_i + qD_{it} + 1 + qR_sI/kT}. \quad (22)$$

As can be seen from Equation (22), the effect of c_2 is also neglected here. From Equations (17) and (21), it follows that

$$\frac{C_{LF}}{C_{HF}} = \frac{(q\epsilon_sN_A/2\psi_s)^{1/2} + qD_{it}}{(q\epsilon_sN_A/2\psi_s)^{1/2}}$$

$$D_{it} = (q\epsilon_sN_A/2\psi_s)^{1/2}(C_{LF} - C_{HF})qC_{HF}. \quad (23)$$

This expression for D_{it} (Equation (23)) is the same as that obtained in Ref.[11] although a different approach was followed. The approach followed in the present work is simpler and the expression for capacitance derived here are more accurate (Section 4) than those in Ref.[11]. The difference between the present approach and the approach of Ref.[11] is in taking into account the influence of the charge in interface states on the dc surface potential for both cases — C_{HF} and C_{LF}. Equation (23) is the basis of the capacitance technique for the determination of interface state density and is easily obtained from Equations (17) and (21). Substituting the values of c_1, c_2 from Equation (6), the expressions are of C_{HF} and C_{LF} are

$$C_{HF} = \frac{[q\epsilon_s N_A/2\psi_s]^{1/2}}{\delta(q\epsilon_s N_A/2\psi_s)^{1/2}/\epsilon_i + 1 + qR_s I/kT + q^2\delta D_{it}/\epsilon_i} \quad (24)$$

$$C_{LF} = \frac{[q\epsilon_s N_A/2\psi_s]^{1/2} + qD_{it}}{\delta(q\epsilon_s N_A/2\psi_s)^{1/2}/\epsilon_i + 1 + qR_s I/kT + q^2\delta D_{it}/\epsilon_i} \quad (25)$$

A comparison of Equation (24) with Equation (18) shows the presence of an extra term $q^2\delta D_{it}/\epsilon_i$ (*i.e.* C_{it}/C_i) in the denominator of Equation (24) which is solely due to the appearance of parameter c_2 in Equation (17). The role of this extra term is quite significant in the C_{HF}–V plots as shown in Fig. 2.

The interface state density can also be measured by the multifrequency admittance method[12,13].

4. RESULTS AND DISCUSSION

In order to establish the physical validity of the present model, the experimental results of Al–pSi Schottky diode from Ref.[5] have been used. The diode series resistance was extracted[18] from the I–V plot. The method in Ref.[19] was applied to determine the variation of $\psi_s(V)$ with the applied bias voltage. The multifrequency admittance method[5,12,13] has been used to obtain the variation of interface state density with the applied voltage.

The experimental high frequency (1 MHz) C–V plot is shown in Fig. 2. Two theoretical C–V plots are also shown in the same figure for comparison with the experimental plot, one using Equation (17) and the other using Equation (18) from Ref.[11]. It is observed that the theoretical curve of Equation (17) is more closer to the experimental curve than its counterpart *i.e.* theoretical curve of Equation (18).

Using the experimental plots for C_{HF} *vs* V (Fig. 2) and D_{it} *vs* V (from multifrequency admittance method) and Equation (23), the experimental low frequency capacitance C_{LF} *vs* voltage plot is obtained. Theoretical low frequency C–V plots corresponding to Equations (21) and (22) are then compared with the experimental C_{LF} *vs* V plot in Fig. 3 for Al–pSi Schottky diode. The results in Fig. 3 clearly indicate that the theoretical C_{LF} *vs* V plot of Equation (21) is more closer to the experimental plot than the theoretical plot of Equation (22).

Figure 4 shows the variation of interface state density with the applied voltage as obtained by the multifrequency admittance method. Making use of the theoretical C_{HF} *vs* V plot and C_{LF} *vs* V plot corresponding to Equations (17) and (21), the variation of D_{it} with voltage is computed, applying the capacitance technique and the results are included in Fig. 4.

Similarly, another theoretical plot of D_{it} *vs* V obtained from the C–V relations of Ref.[11], is shown in Fig. 4 for comparison. The good agreement between the experimental plot and the theoretical plot obtained from the present model assures that the capacitance technique for the determination of interface state density is almost as accurate as the multifrequency admittance method and even much more simpler.

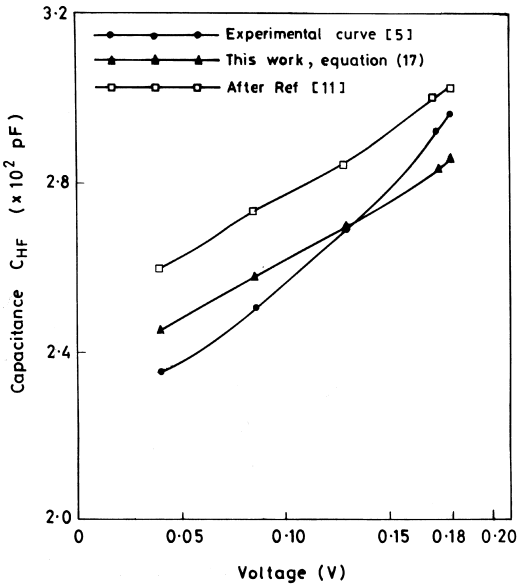

Fig. 2. Experimental and theoretical high frequency capacitance–voltage plots

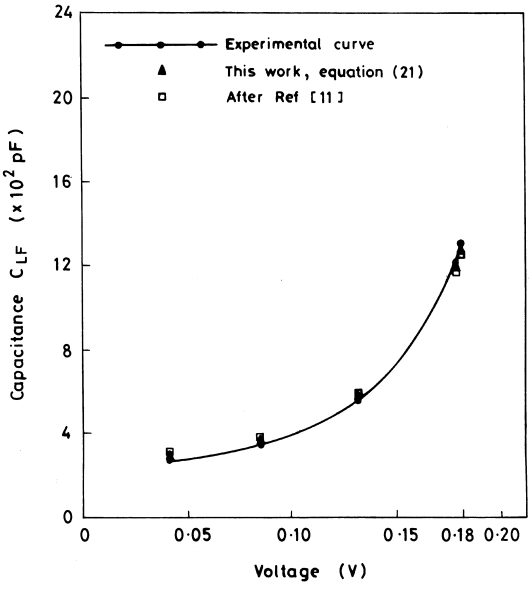

Fig. 3. Experimental and theoretical low frequency capacitance–voltage plots

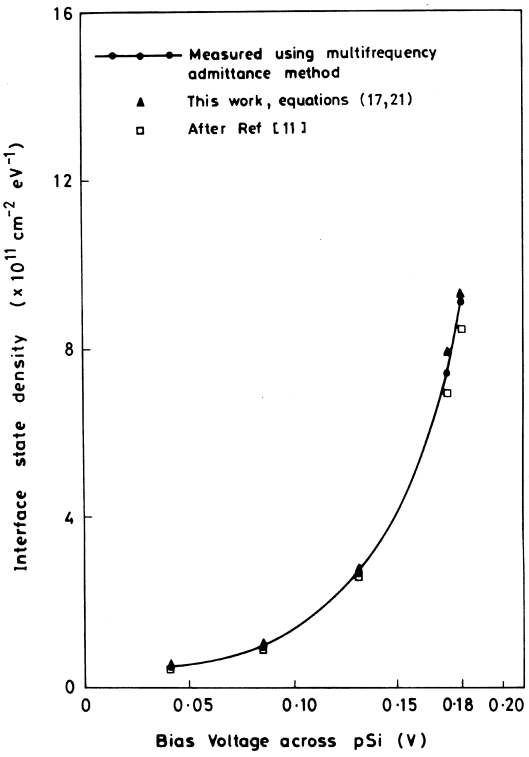

Fig. 4. Comparison between the interfacial state density measured by the multifrequency admittance method and those extracted by the capacitance technique using the above equations

This work primarily discusses the importance of the parameter c_2 in Equations (9), (10), (17) and (21)). Because the series resistance effect is negligible at low current densities, we concentrated on the C–V plots only upto a maximum forward voltage of 0.18 V. A careful observation of the plots in Fig. 2 reveals that the theoretical curve corresponding to Equation (17) is more closer the experimental curve at low voltages than that corresponding to Equation (18) obtained from Ref.[11]. Due to the presence of R_s, the experimental C_{HF}–V curve exhibits a peak of a voltage greater than 0.18 V. In the voltage range of 0–0.18 V, the effect of c_2 is more prominent than the series resistance term and the theoretical values of C_{HF} have been computed using Equation (17) and Equation (18) neglecting the term involving R_s. Because of the nonavailability of R_s value in Ref.[5], the theoretical calculations were restricted up to 0.18 V but it should be noted that Equation (17) and Equation (18) can be used for capacitance calculation even at higher voltages ($V > 0.18$ V) as they take care of the series resistance effect also. A similar agreement of the experimental (C_{LF}–V) plot with theoretical plot using Equation (21) is shown in Fig. 3.

The nature of the variation of interface state density is similar to that obtained in Ref.[5] showing an initial flat region followed by a sharp rise with voltage. Also, the values of D_{it} are approximately of the order of 10^{15} eV/m^2 which agrees well with Tseng and Wu[5]. If the order of D_{it} is even higher *i.e.* 10^{18}–10^{17} eV/m^2 (as in Ref.[2,15]), then the effect of the parameter c_2 in Equations (9), (10), (17) and (21)) will be more prominent. In such cases, the negligence of c_2 in the low and high capacitance expressions can cause appreciable deviation of the theoretical C–V plots from the experimental plots.

5. CONCLUSION

This work presents more accurate low frequency and high frequency capacitance expressions for Schottky barrier diodes as compared to those derived by previous workers. In order to validate our model, the theoretical C–V plots are compared with the available experimental results. A quantitative analysis of the capacitance expressions at low and high frequency has been carried out. The simulated results indicate that the present model explains the experimental results satisfactorily. Here, we determined the variation of surface potential with bias voltage using the method of Ref.[19]. This method was used here because of its simplicity though a more precise assessments of the surface potential could be carried out using other available techniques. An attempt was made to verify the capacitance technique for the determination of interface state density. A comparison of D_{it} values obtained by the capacitance technique with those obtained by the multifrequency admittance method shows that the capacitance technique presented in this work is simple, reliable and as accurate as any other method for the determination of interface state density.

REFERENCES

1. P. K. Vasudev, B. L. Mattes, E. Pietras and R. H. Bube, *Solid-State Electron.* **19,** 557 (1976).
2. A. M. Cowley and S. M. Sze, *J. Appl. Phys.* **36,** 3212 (1965).
3. H. C. Card and E. H. Rhoderick, *J. Phys D Appl. Phys.* **4,** 1589 (1971).
4. A. Deneuville, *J. Appl. Phys.* **45,** 3079 (1974).
5. H. H. Tseng and C. Y. Wu, *Solid-State Electron.* **30,** 383 (1987).
6. S. F. Guo, *Solid-State Electron.* **15,** 537 (1984).
7. E. H. Nicollian and A. Goetzberger, *Bell Syst. Tech J.* **46,** 1055 (1976).
8. J. Werner, A. F. Levi, R. T. Tung, M. Anzlowar and M. Pinto, *Phys. Rev. Lett.* **60,** 53 (1988).
9. P. Chattopadhyay and B. Raychaudhuri, *Solid-State Electron.* **35,** 875 (1992).
10. P. Chattopadhyay and B. Raychaudhuri, *Appl. Surf. Sci.* **78,** 233 (1994).
11. P. Chattopadhyay, *Solid-State Electron.* **39,** 1491 (1996).
12. C. Barret and A. Vapaille, *Solid-State Electron.* **18,** 25 (1975).

13. F. Chekir, C. Barret and A. Vapaille, *J. Appl. Phys.* **54,** 6476 (1983).
14. S. M. Sze, *Physics of Semiconductor Devices,* 2nd ed., p. 301. Wiley (1981).
15. P. Chattopadhyay and A. N. Daw, *Solid-State Electron.* **29,** 555 (1986).
16. J. Szatkowski and K. Sieranski, *Solid-State Electron.* **35,** 1013 (1992).
17. J. Werner, K. Ploog and H. J. Quisser, *Phys. Rev. Lett.* **57,** 1080 (1986).
18. E. Ayyildiz, Turut, Efeoglu, Tuzemen Saglam, Yogurtcu, *Solid St. Electron.* **39**, 83 (1996).
19. P. Chattopadhyay, *Solid-State Electron.* **38,** 739 (1995).
20. A. Turut, N. Yalcin and M. Saglam, *Solid-State Electron.* **35,** 835 (1992).